

Interesting possibilities . . .

Phanish Suryanarayana



QM/MM and ab initio Molecular Dynamics Summer School
Institute for Computational Molecular Science Education

Non-traditional symmetries: cyclic+helical

- Traditional formulations restricted to translational symmetry, i.e., crystals
- **Cyclic and helical symmetry?**
 - Nanostructures such as nanotubes, nanowires, and proteins.
 - Application of mechanical deformations such as bending and torsion.

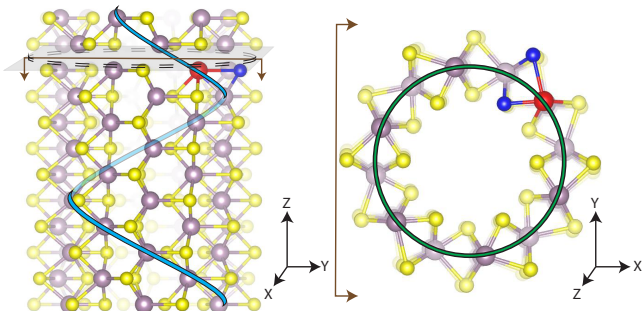


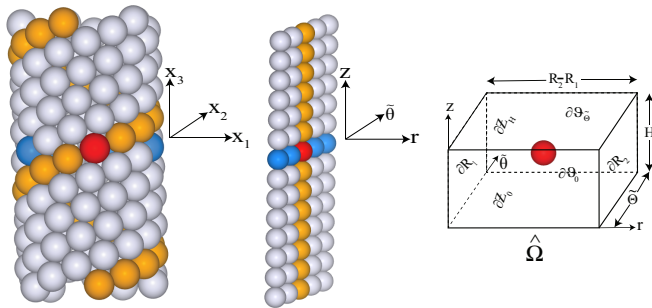
Illustration showing the cyclic and helical symmetry present in a twisted (6,6) TMD nanotube with 2H-t symmetry.

- Can have large number of atoms, e.g., (57,57) MoS₂ nanotube (diameter ~ 10 nm) with an external twist of 2×10^{-4} rad/Bohr has 234,783 atoms in the simulation domain when employing periodic boundary conditions.

Cyclic+helical symmetry-adapted DFT

- Developed a cyclic and helical symmetry-adapted formulation of DFT.

(Sharma and Suryanarayana, 2021)

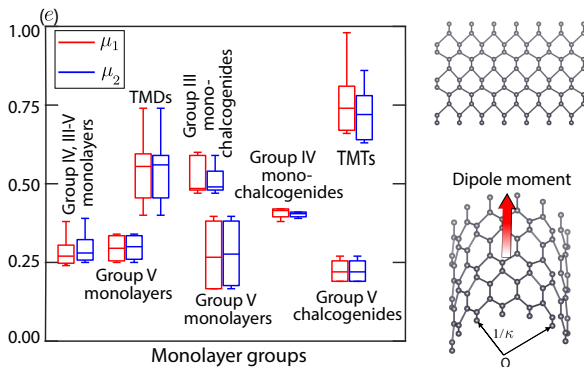


Left: Illustration of a nanotube structure in Cartesian coordinates. Middle: Nanotube in helical coordinates. Right: Fundamental domain for the nanotube.

- Electrostatics: structural symmetry
- Kohn-Sham eigenproblem: electronic symmetry, i.e., cyclic and helical Bloch's theorem
- A number of applications, including flexoelectricity, strain engineering, ...!

2D materials: Flexoelectric effect

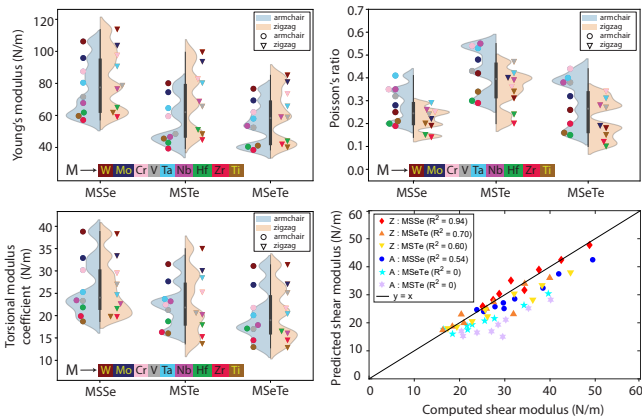
- Coupling between dipole moment/polarization and strain gradient.
- Novel formulation for the calculation of the transversal flexoelectric coefficient (Codony et. al., 2021)
- Calculated the transversal flexoelectric coefficient for different groups of 2D materials (Kumar et. al., 2021).



Janus TMD nanotubes: Elastic properties

- Calculated the elastic properties of Janus TMD nanotubes

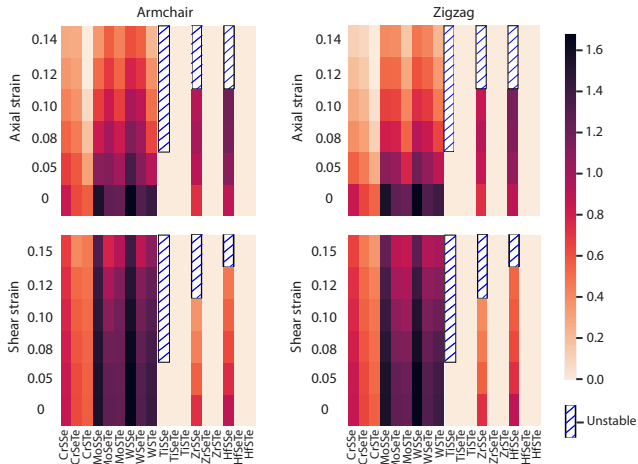
(Bhardwaj, and Suryanarayana, 2022).



- Observed isotropic-type behavior
- Use in higher-scale models

Janus TMD nanotubes: Strain engineering

- Effect of axial and torsional deformations on the electronic properties of Janus TMD nanotubes (*Bhardwaj and Suryanarayana, 2022*)



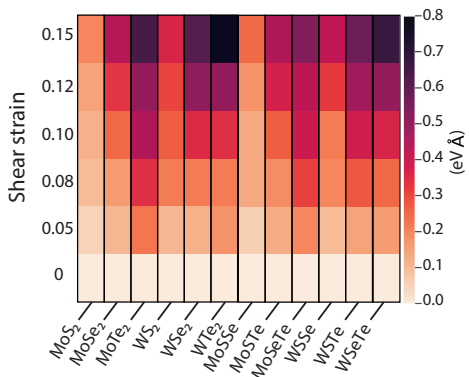
Variation of bandgap with axial and torsional deformations for TMD nanotubes.

- Insulator to metal transitions.

Janus TMD nanotubes: Spintronics

- Spintronics: Exploitation of both spin and the electronic charge in solid state devices
- Zeeman and Rashba effects: splitting of the electronic bands along the energy and wavevector axes, respectively.
- Relativistic effects arising from spin-orbit coupling (SOC).
- Effect of axial and torsional deformations in Janus TMD nanotubes

(Bhardwaj and Suryanarayana, 2024).



Variation in the Rashba splitting coefficient with torsional deformations.

- Diagonalization: Cost $\mathcal{O}(N^3)$, Memory $\mathcal{O}(N^2)$

Idea

- Get rid of the orbitals, with no loss in accuracy
- Directly evaluate the electron density and quantities of interest such as energy, force, and stress
- Employ nearsightedness principle!

- A number of previous efforts for the development of $\mathcal{O}(N)$ methods

Limitations

- Suitable mainly for insulating systems
- Systematically improvable accuracy?
- Large-scale parallelization?

Density matrix formulation

- Kohn-Sham DFT can be reformulated in terms of the density matrix

Free Energy

$$\mathcal{E}(\mathcal{D}, \mathbf{R}) = \text{Tr} \left(-\frac{1}{2} \nabla^2 \mathcal{D} \right) + E_{xc}(\rho_{\mathcal{D}}) + E_{el}(\rho_{\mathcal{D}}, \mathbf{R}) - TS(\mathcal{D})$$

where

\mathcal{D} : Density operator/matrix, Electron density: $\rho_{\mathcal{D}}(\mathbf{x}) = 2\mathcal{D}(\mathbf{x}, \mathbf{x})$

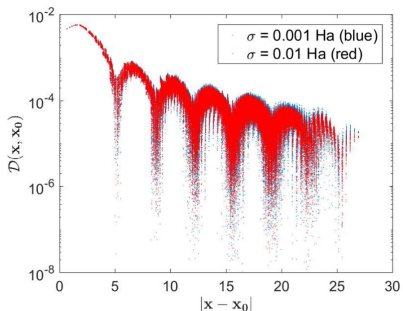
Variational problem

$$\mathcal{D}^* = \left\{ \arg \inf_{\mathcal{D}} \mathcal{E}(\mathcal{D}, \mathbf{R}) \quad \text{s.t.} \quad 2\text{Tr}(\mathcal{D}) = N_e \right\}$$

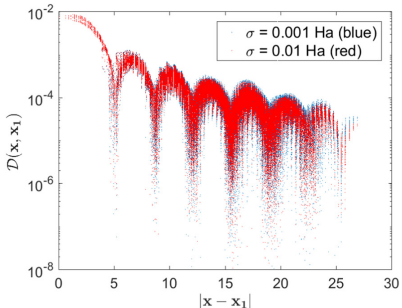
Euler-Lagrange equation

$$\mathcal{D} = g(\mathcal{H}, \mu, \sigma) = \left(1 + \exp \left(\frac{\mathcal{H} - \mu \mathcal{I}}{\sigma} \right) \right)^{-1} = \sum_n g_n |\psi_n\rangle \langle \psi_n|$$

Nearsightedness principle: decay of density matrix



(a) $x_0 = [0.00 \ 0.00 \ 0.00] \text{ Bohr}$



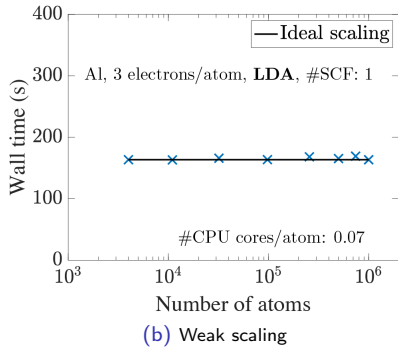
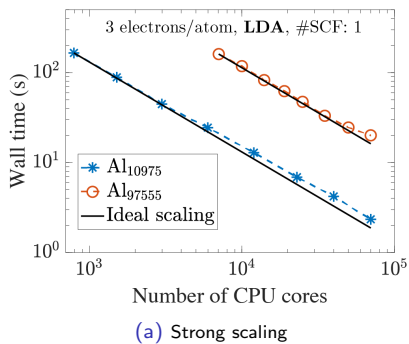
(b) $x_1 = [3.89 \ 3.89 \ 3.89] \text{ Bohr}$

Decay of the density matrix in aluminum (*Suryanarayana, 2017*)

- Exponential decay in insulators and metals at finite temperature
- Exploit decay to develop $\mathcal{O}(N)$ methods
- Spectral Quadrature (SQ) method: quadrature in the spectrum of the nodal density matrix (*Suryanarayana, 2013*)

Spectral Quadrature (SQ) method

- $\mathcal{O}(N)$ DFT applicable to both insulating and metallic systems



- System sizes up to a million atoms! (Gavini et. al., 2023)
- Large prefactor at ambient conditions due to the large grid points/atom (400 – 30,000)
- Large number of applications at high-temperatures (e.g. warm dense matter)

Motivation

- Warm dense matter (WDM) generally inaccessible to Kohn-Sham DFT calculations.

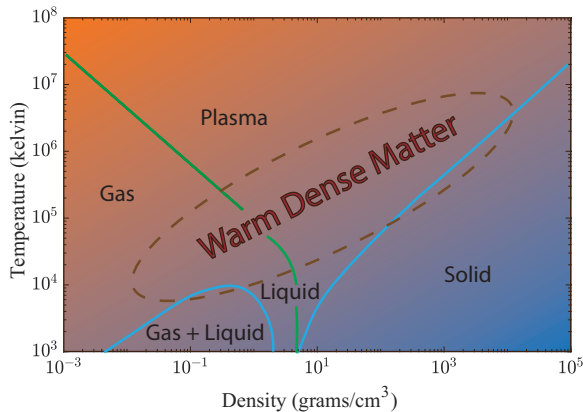
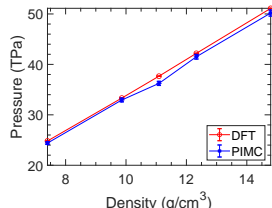


Illustration of the WDM regime. The shading of blue/orange indicates the relative importance of quantum mechanical/classical effects.

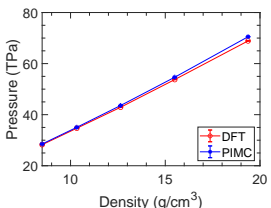
(Adapted from *Report of the Workshop on High Energy Density Laboratory Physics Research Needs, November 2019.*)

SQDFT: Comparison with PIMC

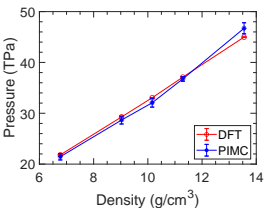
- Equation of state (EOS) calculations through AIMD simulations.



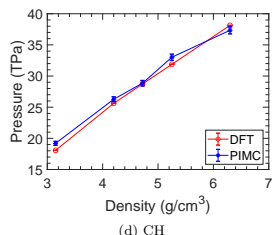
(a) B



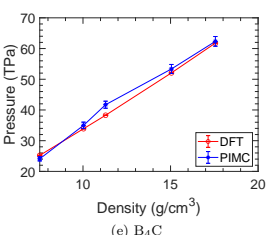
(b) C



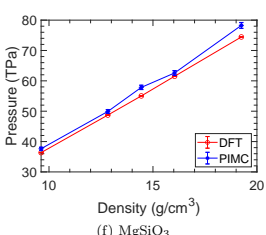
(c) BN



(d) CH



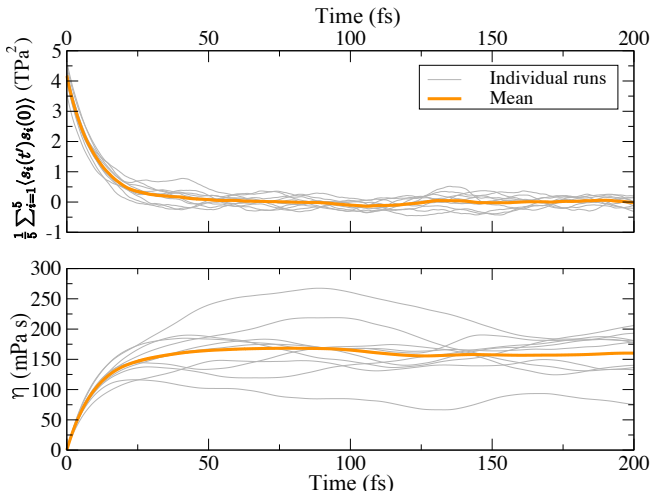
(e) B₄C



(f) MgSiO₃

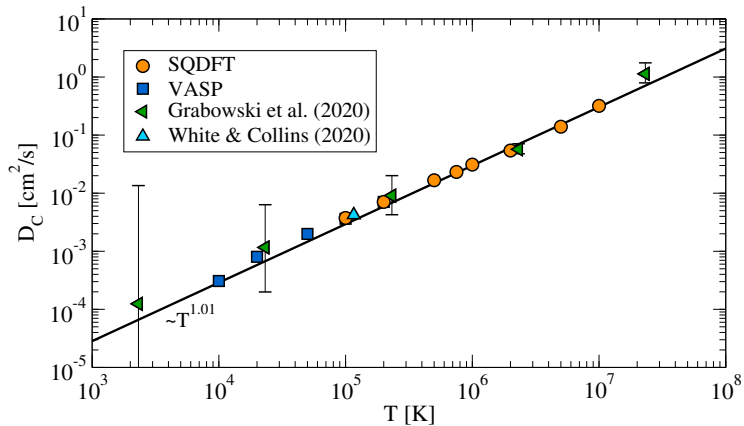
Comparison of SQDFT and PIMC. Temperatures around a million kelvin.

SQDFT: Application to Hydrogen



Ensemble average (top) and viscosity (bottom) for hydrogen at 1 million K and density 2 g/cm³
(Sharma et. al., 2020)

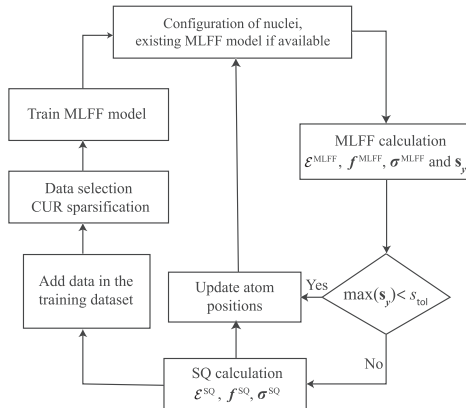
SQDFT: Application to Carbon



Diffusion coefficient for carbon (Bethkenhagen et. al., 2023)

On-the-fly MLFF MD

- Machine learned force field (MLFF) trained during the MD.
- SOAP descriptors, kernel method, and Bayesian linear regression
- Initial few DFT steps.
- DFT steps performed when the Bayesian error estimate exceeds a threshold



Outline of the on-the-fly MLFF framework.

Structure of molten $\text{Al}_{0.88}\text{Si}_{0.12}$

- Δ -machine learning with respect to orbital-free DFT (OF-DFT)

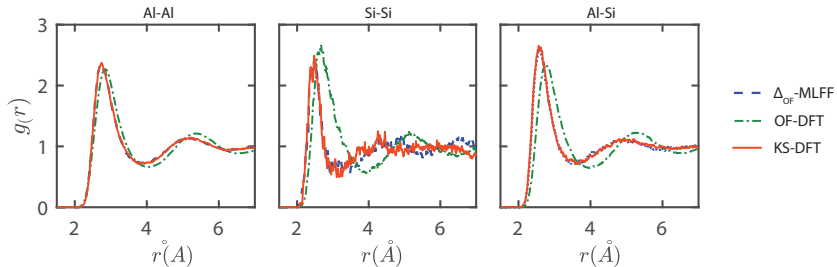
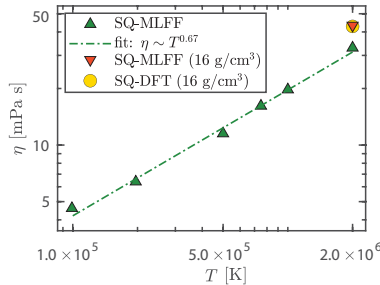
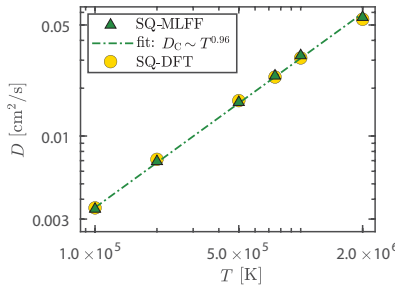


Fig: Pair distribution functions for the molten $\text{Al}_{0.88}\text{Si}_{0.12}$ alloy at 1473 K, as computed by $\Delta_{\text{OF}}\text{-MLFF}$, OF-DFT, and KS-DFT. (Kumar et. al., JCP, 2023)

Accuracy of SQ-MLFF

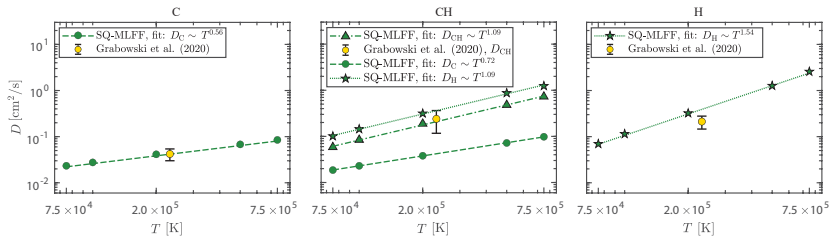
- Ionic transport properties: diffusion coefficient (D) and shear viscosity (η)
- Comparison with DFT results.



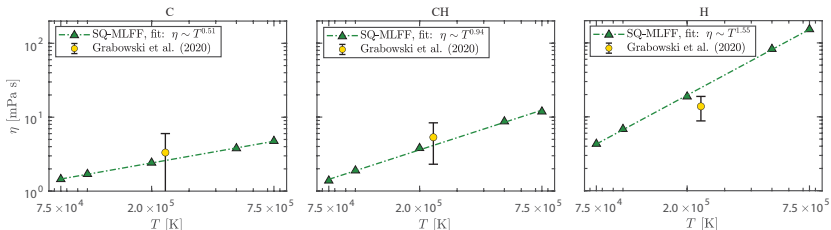
Carbon at a density of 10 g/cm³ (Kumar et. al., 2024).

- Power law with temperature.
- Excellent agreement between SQ-MLFF and DFT.
- Agreement extends to equation of state calculations.

Diffusion and viscosity of CH, C, and H



Diffusion coefficients vs temperature for CH, C, and H, all at a density of 1 g/cm³



Viscosity vs temperature for CH, C, and H, all at a density of 1 g/cm³

Performance of MLFF

- MD simulations with 500,000 steps

T [K]	# MD steps		Time [CPU s]		Speedup
	MLFF	SQ	MLFF	SQ	
100,000	499,694	306	17	7×10^5	1339
200,000	499,720	280	14	1×10^5	1246
500,000	499,724	276	10	4×10^4	1134
750,000	499,776	224	10	2×10^4	979
1,000,000	499,807	193	7	1×10^4	940
2,000,000	499,890	110	7	1×10^4	976

Variation of SQ-MLFF performance with temperature for C at a density of 10 g/cm³. The timings are per MD step, as averaged over the entire simulation.

- Up to three orders of magnitude speedup by SQ-MLFF.
- Speedup increases with number of MD steps
- Nearly all the DFT steps (i.e., training) happens towards the beginning of the simulation.

Concluding remarks

- SPARC is an accurate, efficient, and scalable open-source electronic structure code.
- Many advanced features, able to efficiently leverage moderate and large-scale computational resources alike.
- Straightforward to install, use, and modify, with minimal external library dependencies.
- An **order of magnitude faster than state-of-the-art planewave codes**, with a range of exchange-correlation functionals, and with increasing advantages as the number of processors is increased.
- SPARC efficiently scales to thousands of processors in regular operation, bringing solution times down to about **a minute for systems with $O(500\text{-}1000)$ atoms**, and **a few seconds for $O(100\text{-}500)$ atoms**.
- GPU acceleration: **diagonalization speedup of 5–12x**. Public release soon.
- **Cyclic+helical symmetry adaption**. Efficient study of nanostructures/nanomaterials and their response to mechanical deformations.
- **$O(N)$ SQ method**, it has been scaled to system sizes of over a **million atoms**.
- **Study of warm dense matter (WDM)**

Acknowledgements

- Qimen Xu, Xin Jing, Abhiraj Sharma, Boqin Zhang, Swarnava Ghosh, Phanisri P. Pratapa, Shashikant Kumar, Mostafa F. Shojaei, David Codony, Sayan Bhowmik
- John E Pask (LLNL), Edmond Chow (GT), Andrew J. Medford (GT), Amartya Banerjee (UCLA)
- Hua Huang, Shikhar Shah, Lucas Erlandson, Benjamin Comer
- **U.S. Department of Energy (DOE), Office of Science**
U.S. Department of Energy (DOE), National Nuclear Security Administration (NNSA): Advanced Simulation and Computing (ASC) Program
U.S. National Science Foundation (NSF)

Thank You!
Questions?